Ryan Pekarek[1,2], Steven S. Christensen[3], Jun Liu[2], and Nathan R. Neale[2]

[1]Department of Chemistry, University of Texas at Austin
[2]Chemistry and Nanoscience Center, National Renewable Energy Laboratory
[3]Materials Science Center, National Renewable Energy Laboratory

Hybrid Molecular/Inorganic Modification of Nanoporous Black Silicon

Inspiration and Project Goals

Hybrid Molecular/Inorganic Surface Modification

- Organic monolayers shift HER onset via the molecular dipole
- Deposition of metal oxides (Al_2O_3, TiO_2) leads to considerable positive shifts in V_{onset}

Nanoporous Black Silicon

- Nanotextured surface affords significantly increased photocurrent (30-40 mA/cm^2)
- Positive onset potentials after ambient oxidation

Objective

- Understand the effect of molecular dipoles and oxide layers on textured semiconductor surfaces

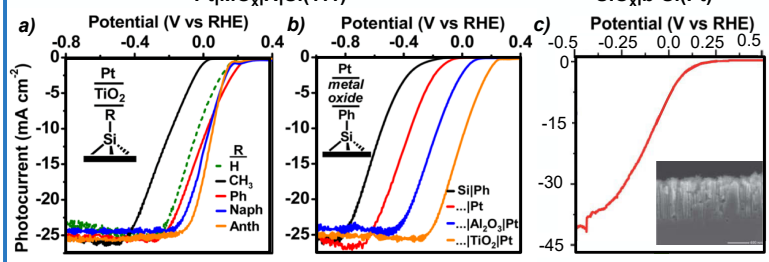

Seo, J.; Kim, H. J.; Pekarek, R. T.; Rose, M. J. *J. Am. Chem. Soc.* 2015, 137 (9), 3173–3176.

Zhao, Y.; Anderson, N. C.; Neale, N.R. et. al. *Nano Lett.* 2015, 15 (4), 2517–2525.

Figure 1. Current-voltage scans of the inspiration for this work: hybrid molecular/inorganically treated planar Si(111) where the (*a*) organic monolayer and (*b*) metal oxide is varied; (*c*) oxidized black silicon with buried Pt nanoparticles.

Constructing the Interface

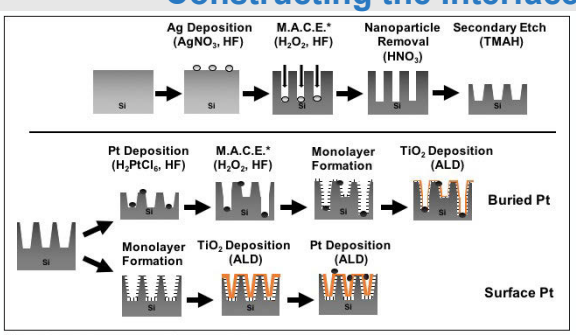

*M.A.C.E. – Metal Assisted Chemical Etch

Planar Si

Black Si

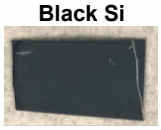

Figure 2. Scheme depicting the synthetic steps in this work[1]: silicon nanotexturing (top), monolayer formation and oxide deposition (bottom). Photos of treated (planar) and untreated (black) wafers are shown to the right.

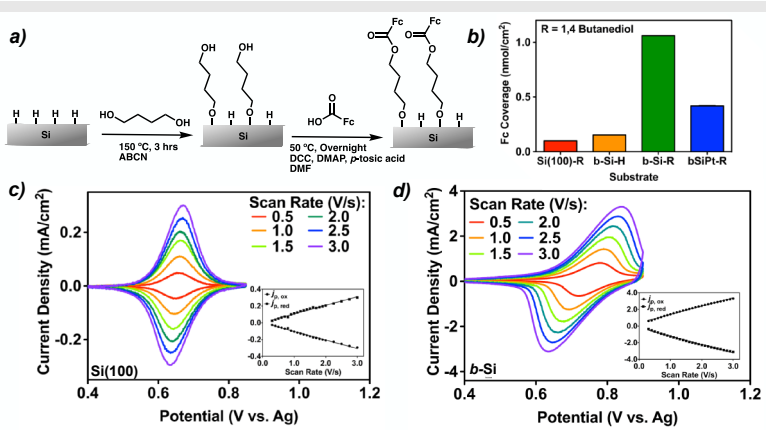

Figure 3. Confirming monolayer formation: *a)* Scheme depicting the the incorporation of ferrocenecarboxylic acid into the monolayer to confirm successful formation. *b*) Electrochemically measured coverage values for planar Si(100), etched *b*-Si (control), and the diol functionalized *b*-Si wafers with and without buried Pt. *c-d*) Cyclic voltammograms of ferrocenecarboxylic acid-modified substrates: planar Si(100) (*c*) and b-Si (*d*).

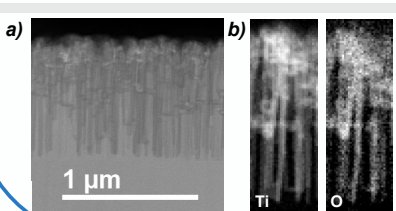

Figure 4. Imaging TiO_2 in the Pores:
Cross section of *b*-Si-*R* pores after 200 cycles of TiO_2 ALD (atomic layer deposition).
a) Dark-field TEM image
b) Ti and O element maps of the pores

Observations:

- Pores are ~750-800 nm deep, 40-50 nm wide
- Little space between pores (10-50 nm)
- TiO_2 deposits into entire length of pore and forms a layer at the top

Effects of Surface Modification

Measuring Flatband Potential via IMHFR

- Flatband potential (E_{fb}) governs the driving force for photoelectrochemical reactions
- *Intensity Modulated High Frequency Resistivity*[2] (IMHFR) measures the light and dark space-charge region resistance (R_{SC}) as a function of potential
- E_{fb} is the most positive (for *p*-Si) potential where R_{light} and R_{dark} are significantly different
- High frequency impedance measurement effectively 'shorts' surface states from oxides or defects

Monolayer Composition and E_{fb}

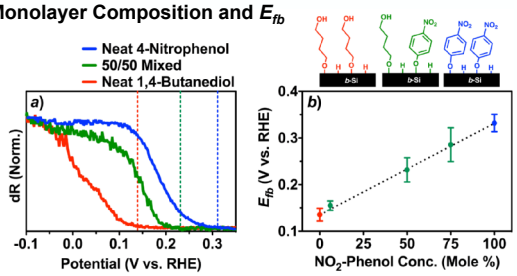

Figure 5. Monolayer shifting E_{fb}: Addition of 4-nitrophenol (strong positive dipole[3]) shifts E_{fb} positively compared to 1,4-butanediol (neutral dipole).
a) Representative IMHFR voltammograms, varying monolayer composition
b) E_{fb} as a function of nitrophenol concentration in the monolayer growth solution

Interface Architecture and E_{fb}

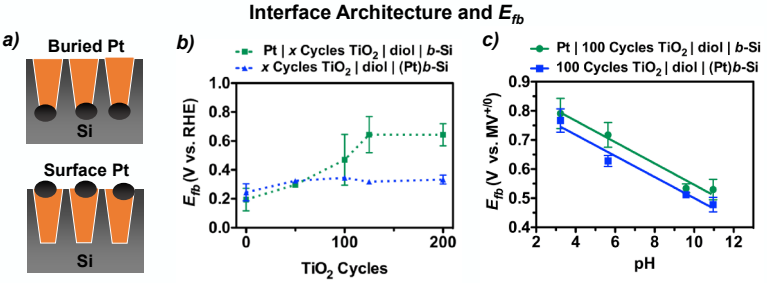

Figure 6. Inorganic layers and E_{fb}: *a*) Scheme depicting two interface structures: Pt buried via chemical etch, and Pt deposited onto the oxide via ALD. *b*) E_{fb} as a function of TiO_2 deposition cycles for both architectures. *c*) Fermi pinning experiment; E_{fb} as a function of solution pH.

- TiO_2 shifts E_{fb} positively when Pt is placed on the TiO_2 while remaining relatively constant when Pt is buried
- Constant E_{fb} is not due to the Pt pinning the band edge, as shifts with pH still occur
- Buried Pt nanoparticle likely 'shunts' the interface, negating the effect of TiO_2 layer

Buried Pt Voltammetry

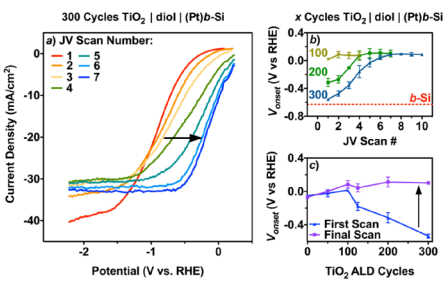

Figure 7. JV Curves of TiO_2 | *R* | *b*-Si(Pt*)*:
a) Repeated voltammograms of a 300 TiO_2 cycle sample. V_{onset} shifts positively and max current stabilizes.
b) V_{onset} as a function of scan number for multiple TiO_2 thicknesses
c) V_{onset} for the first and stabilized scan as a function of TiO_2 ALD cycles

- Pt nanoparticle is effectively separated from the solution after 300 ALD cycles
- Activity recovered after repeated scanning at negative potentials, likely due to electrochemical etching of the TiO_2

Voltammetry and Interface Architecture

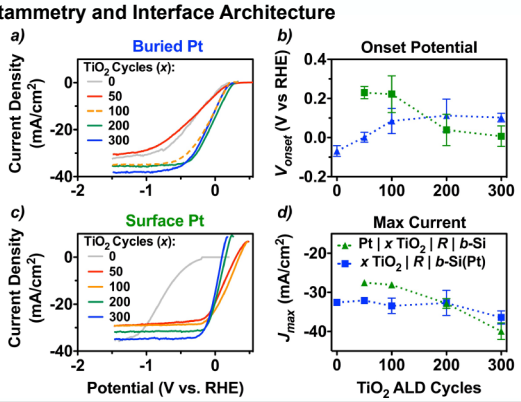

Figure 8. JV behavior of surface studied in this work (*R* = diol):
Voltammograms:
a) b-Si(Pt)-*R*|TiO_2 after scanning
c) b-Si-R|TiO_2|Pt

Results: V_{onset} (b) and max current, J_{max}, (*d*) vs TiO_2 thickness.

- Surface Pt samples shown most positive V_{onset}, decreasing with TiO_2
- Buried Pt samples improve with additional TiO_2
- Both architectures show slight increase in J_{max} when TiO_2 is thick, possibly due to additional anti-reflectivity of TiO_2

Future Studies

- Voltammetric characterization of surfaces varying monolayer composition
- Durability of samples as a function of interfacial architecture (TiO_2 thickness and Pt location)

This work was supported by the U.S. Department of Energy, Office of Science, Office of Basic Energy Sciences, Division of Chemical Sciences, Geosciences, and Biosciences, Solar Photochemistry Program under contract number DE-AC36- 08GO28308 to NREL. RTP was supported by the the Science Graduate Student Research (SCGSR) fellowship program administered by the Oak Ridge Institute for Science and Education (ORISE) for DOE under contract number DE-SC0014664.

U.S. DEPARTMENT OF ENERGY | Office of Science

1) Aguiar, J.A.; Anderson, N.C.; Neale, N.R. *J. Mater. Chem. A*, **2016**, 4, 8123.
2) Anderson, N.C.; Carroll, G.M.; Pekarek, R.T.; Neale, N.R. *J. Phys. Chem. Lett.* **2017**, 8, 5253-5258.
3) Iyer, A.; Kearney, K.; Wakayama, S.; Odoi, H.; Ertekin, E. *Langmuir.* **2018**, 34, 2959.